Eurasian autumn snow link to winter North Atlantic Oscillation strongest for Arctic warming periods

Martin Wegmann (1), Marco Rohrer (2,3,*), María Santolaria-Otín (4) and Gerrit Lohmann (1)

(1) Alfred Wegener Institute, Helmholtz Centre for Polar and Marine Research, Bremerhaven, Germany

(2) Oeschger Centre for Climate Change Research, University of Bern, Bern, Switzerland

(3) Institute of Geography, University of Bern, Bern, Switzerland

(4) Institut des Géosciences de l'Environnement, Université Grenoble-Alpes, France

(*) now at: Axis Capital, Zurich, Switzerland

Abstract:

In recent years, many components of the connection between Eurasian autumn snow cover and wintertime North Atlantic Oscillation (NAO) were investigated, suggesting that November snow cover distribution has strong prediction power for the upcoming Northern Hemisphere winter climate. However, nonstationarity of this relationship could impact its use for prediction routines. Here we use snow products from long-term reanalyses to investigate interannual and interdecadal links between autumnal snow cover and atmospheric conditions in winter. We find evidence for a negative NAO-like signal after November with a strong west-to-east snow cover gradient, which is valid throughout the last 150 years. This correlation is linked with a consistent link of November snow to the stratospheric polar vortex state. Nevertheless, interdecadal variability for this link shows episodes of decreased correlation strength, which co-occur with episodes of low variability in the November snow index. On the contrary, periods with high prediction skill for winter NAO are found in periods of high November snow variability, which co-occur with the Arctic warming periods of the 20th century, namely the early 20th century Arctic warming between 1920-1940 and the ongoing anthropogenic global warming at the end of the 20th century. A strong snow dipole itself is consistently associated with reduced Barents-Kara sea ice concentration, increased Ural blocking frequency and negative temperature anomalies in eastern Eurasia.

Keywords: SNOW, NAO, SEA ICE, VARIABILITY, PREDICTION

1. Introduction

As the leading climate variability pattern affecting winter climate over Europe (**Thompson and Wallace 1998**), the North Atlantic Oscillation (NAO) has been extensively studied over the last decades (**Wanner et al., 2001; Hurrell and Deser 2010; Moore and Renfrew 2012; Pedersen et al., 2016; Deser et al., 2017**). The NAO has been defined as the variability of the pressure gradient between Iceland (representing the edge of the polar front) and the Azores (representing the subtropical high ridge). The sign of the NAO is related to weather and climate patterns stretching from local to continental scales. Since its variability has severe socioeconomic, ecological and hydrological impacts for adjacent continents, seasonal to decadal predictions of the state of the winter NAO are high–priority research for many climate science centers (**Jung et al., 2011; Kang et al., 2014; Scaife et al., 2014; Scaife et al., 2016; Smith et al., 2016; Dunstone et al., 2016; Wang et al., 2017; Athanasiadis et al., 2017**).

Together with the rapid warming of the Arctic and the increased frequency of severe winters over Eurasia and North America (**Yao et al., 2017; Cohen et al., 2018; Kretschmer et al., 2018; Overland and Wang 2018**), recent studies highlighted the state of the Northern Hemispheric cryosphere as a useful predictor for the boreal wintertime (DJF) NAO (**Cohen et al., 2007; Cohen et al., 2014; Vihma 2014; Garcia-Serrano et al., 2015; Cohen 2016, Orsolini et al., 2016; Crasemann et al., 2017; Warner 2018**). Although both systems seem to be connected (**Cohen et al., 2014; Furtado et al., 2016; Gastineau et al., 2017**), the emerging main hypothesis connects reduced autumn Barents-Kara sea ice concentration and increased Siberian snow cover with a negative NAO state in the following winter months (**Cohen et al., 2014**).

The proposed mechanism behind this hypothesis is a multi-step process, starting with autumn sea ice loss for the European Arctic, followed by altered tropospheric circulation due to elevated Rossby wave numbers, vertical propagation of said Rossby waves upward into the stratosphere and consequently a weakening of the polar vortex (see **Cohen et al., 2014** for an in depth discussion). With the weakening (or the reversal) of the polar vortex, a stratospheric warming signal manifests. This signal propagates slowly back into the troposphere, where it manifests itself as a negative NAO, connected to the concurrent cold winters for Eurasia (**Kretschmer et al., 2018**).

In recent years, many components of this pathway were investigated, especially concerning the increased frequency of cold winters over Europe and the emergence of the counter-intuitive "Warm Arctic – cold continent" (WACC) pattern over Eurasia (**Petoukhov and Semenov 2010; Vihma 2014**). However, there remains substantial uncertainty about the impact of Arctic sea ice in terms of location (**Zhang et al., 2016; Luo et al., 2017; Screen 2017; Kelleher and Screen 2018**), timing (**Honda et al., 2009; Overland et al., 2011; Inoue et al., 2012; Suo et al., 2016; Sorokina et al., 2016; King et al., 2016; Screen 2017; Wegmann et al., 2018a; Blackport and Screen 2019**) or if sea ice can be used as a predictor/forcing at all based on the contrasting result of model studies (**McCusker et al., 2016; Collow et al., 2016; Pedersen et al., 2016; Boland et al., 2017; Crasemann et al., 2017; Ruggieri et al., 2017; Garcia-Serrano et al., 2017; Francis 2017; Screen et al., 2018; Mori et al., 2019; Hoshi et al., 2019; Blackport et al., 2019; Romanowksy et al., 2019**).

The interplay between Arctic sea ice and Siberian snow is much less explored. **Ghatak et al. (2010)** showed that reduced autumn polar sea ice leads to the emergence of increased Siberian winter snow cover, especially so in the eastern part of Eurasia. This dipole signal was amplified in coupled climate model runs for the 21st century, where sea ice is substantially diminished. In an observational study, **Yeo et al. (2016)** point out that the moisture influx from the open Arctic ocean into the Eurasian continent contributes to the increase of snow cover, a mechanism described by **Wegmann et al. (2015)**. **Gastineau et al. (2017)** found that reduced sea ice is connected to a distinct November snow dipole over Eurasia, both in reanalysis and model data. They further state that the snow component is a statistically more powerful predictor than sea ice for the atmosphere in the following winter. This relationship was also found in a range of climate models, albeit with weaker links. **Xu et al. (2019)** found the same correlation in observational and model data, however looking at winter climate only. Based on their analysis, the authors state that the enhanced snow cover in winter is a product of the negative NAO rather than a precursor. **Sun et al. (2019)** highlight the importance of elevated North Atlantic sea surface temperatures for the development of a Eurasian snow dipole in autumn. This warming of the North Atlantic favors reduced sea ice cover for the European part of the Arctic, which triggers a high pressure anomaly over the Northern Ural Mountains via increased ocean to atmosphere heat fluxes, transporting cold air masses towards the south of its eastern flank.

The possible impact of the Siberian snow on the stratosphere and eventually on the NAO is well discussed in **Henderson et al. (2018)**. Although observational NAO prediction studies with Siberian snow showed great success in the past (**Cohen and Entekhabi 1999; Saito et al., 2001; Cohen et al., 2007; Cohen et al., 2014; Han and Sun 2018**), links between snow and the stratosphere still seem to be missing or too weak in model studies (**Furtado et al., 2015; Handorf et al., 2015; Tyrrell et al., 2018; Gastineau et al., 2017; Peings et al., 2017**), whereas nudging realistic snow changes to high resolution models seems to improve the prediction skill (**Orsolini and Kvamsto 2009; Orsolini et al., 2016; Tyrrell et al., 2019**). Moreover, even though the stratosphere–surface connection is now reasonably well established (**Kretschmer et al., 2018**), the timing and location of the snow cover used for the prediction is, as with sea ice, still debated (**Yeo et al., 2016; Gastineau et al., 2017**). As an additional caveat, **Peings et al. (2013)** and more recently **Douville et al. (2017)**, showed that the proposed autumn snow-to-winter NAO relationship is non-stationary for the 20th century. A possible modulator for that relationship might be the phase of the Quasi Biennial Oscillation (QBO) (**Tyrrell et al., 2018; Peings et al., 2017; Douville et al., 2017**). **Peings (2019)** argues that neither snow nor sea ice anomalies trigger the stratospheric conditions needed to produce winter extremes and that instead high tropospheric blocking frequency over Northern Europe leads to the cryosphere anomalies.

Here, we follow up on the definition of a November Eurasian snow cover dipole (**Ye and Wu 2017; Gastineau et al., 2017; Han and Sun 2018)** which was identified to provide predictive power for the following winter months at the end of the 20th century. It is however unclear if this prediction skill is stable for time periods further back than 30 years and how it evolves in periods of high Arctic sea ice cover. In this study we address the question of a) nonstationarity of the Eurasian snow cover to winter European surface climate relationship in the 20th century, b) importance of snow versus sea ice as predictor and c) possible precursors/modulators of the sea ice–snow–stratosphere chain. With this we aim to contribute to the understanding of impacts of cryosphere variability on midlatitude circulation (**Francis 2017; Henderson et al., 2018; Cohen et al; 2019**). To this end, we utilize centennial reanalyses and reconstruction data, where we focus on the transition from October to November to DJF to facilitate the idea of seasonal prediction.

This paper is organized as follows: Section 2 describes the data and methods used. In section 3, we introduce the snow cover indices and their interannual prediction value. Section 4 investigates interdecadal shifts in the correlation between snow cover and NAO as well as

possible determining factors. The results are discussed in section 5 and finally summarized in section 6.

2. Data and Methods

a. Atmospheric reanalyses

To evaluate long-term reanalyses, we use snow cover, snow depth and atmospheric properties from the MERRA2 reanalysis (**Gelaro et al., 2017**). MERRA2 has a dedicated land surface module and was found to reproduce local in-situ snow conditions over Russia very well (**Wegmann et al., 2018b**). For a detailed description of how MERRA2 computes snow properties see e.g. **Orsolini et al., (2019)**.

To cover the 20th century and beyond, we include two long-term reanalyses in this study, namely the NOAA-CIRES 20th century reanalysis Version 2c (20CRv2c) (**Cram et al., 2015**) as well as the Centre for Medium-Range Weather Forecasts (ECMWF) product ERA-20C (**Poli et al., 2016).** From the ERA-20C product we use snow depth, whereas from 20CRv2c we investigate snow depth and snow cover. Both reanalyses were found to represent interannual snow variations over Eurasia remarkably well. For an in-depth discussion of their performance and their technical details concerning snow computation see **Wegmann et al., (2017)**. We also performed the same analysis using the coupled ECMWF reanalysis CERA-20C (**Laloyaux et al., 2018**), but found no added knowledge gain over ERA-20C. Thus, we do not include CERA-20C in any further analysis.

We use detrended anomalies of these three reanalysis products to extend the October and November index proposed by **Han and Sun (2018)** into the past, where the November index is in essence the snow dipole described by **Gastineau et al. (2017)** using maximum covariance analysis (Figure 1). Where the October index is just calculated as field average snow cover, the November index is computed as difference between the eastern and the western field average. It should be noted, that **Han and Sun (2018)** found the November index to be linked to a negative NAO and colder Eurasian near-surface temperatures, whereas the October index was correlated with warmer-than-usual temperatures over Eurasia and a southward-shifted jet. However, since many studies focus on Northern Eurasian October snow cover as the predictor for winter climate, we will include it nonetheless. MERRA2 and 20CRv2c offer snow cover as well as snow depth as a post-process output, however ERA-20C only offers snow depth. We refrain from converting it to snow cover ourselves, but found

the index based on snow depth to be extremely similar (also see Supplementary Figure 1) to the same index using snow cover. Moreover, comparing snow indices from reanalyses with snow indices using the NOAA Climate Data record of Northern Hemisphere Snow Cover extent (**Robinson et al. 2012),** which incorporates satellite data, does not highlight any meaningful differences (Supplementary Figure 2). All snow indices are normalized and linearly detrended with respect to their overall time period. Generally, we found the long term reanalyses to be of comparable quality of MERRA2 during the overlapping periods.

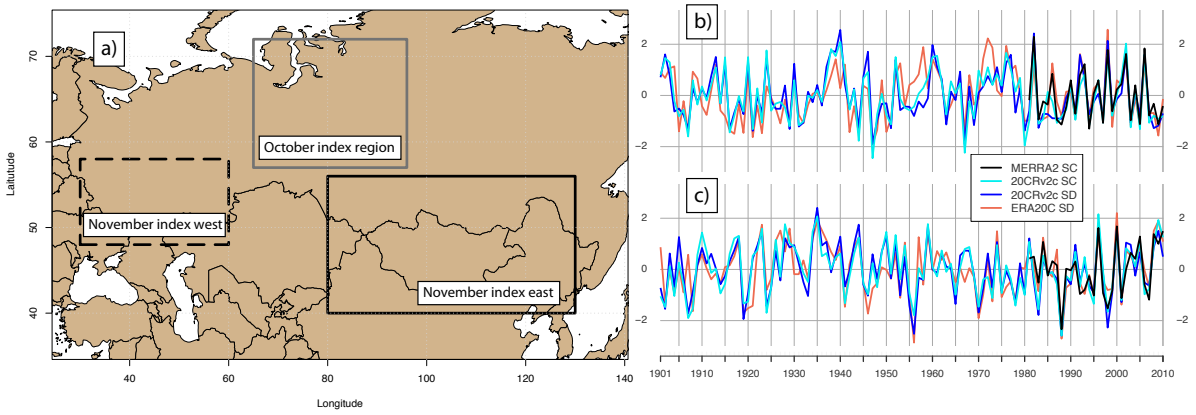

Figure 1: a) Regions for October and November snow index used in this study. b) Linearly detrended and standardized October snow index comparison for the 20th century for snow cover (SC) and snow depth (SD) variables. c) same as b) but for the November snow dipole.

Besides snow properties we use detrended atmospheric and near-surface anomaly fields from all three reanalyses. Moreover, as **Douville et al. (2017)**, we use the field averaged (60°–90° N) 10 hectopascal (hPa) geopotential height (GPH) anomalies in ERA-20C as a surrogate for polar vortex (PV) strength. Although ERA-20C only assimilates surface pressure, correlation between this stratospheric index in ERA-20C and MERRA2 during the overlapping time periods is higher than 0.9.

The ERA20C 10 hPa November–December mean GPH shows remarkable interannual agreement with state-of-the-art reanalyses that assimilate upper air data for the period 1958–2010 (see Supplementary Figure 3). Moreover, MERRA2 and ERA20C 10 hPa GPH anomalies agree best over the northern polar regions with correlation coefficients of >0.9 for the period 1981–2010 (see Supplementary Figure 3). This fact supports the extended value of the ERA20C polar stratosphere. Before 1958, the quality of the ERA20C stratosphere is difficult to assess, but the comparison with reconstructions of 100 hPa GPH zonal means shows very good agreement for late autumn and winter months (see Supplementary Figure 4).

As the 20CRv2c ensemble mean dilutes the interannual variability signal back in time with increased variability within the ensemble members, we use the deterministic run of ERA20C for the following stratosphere analyses.

We use 6-hourly 500 hPa GPH fields (GPH500) to calculate monthly blocking frequencies according to **Rohrer et al. (2018)**. Blockings are computed according to the approach introduced by **Tibaldi and Molteni (1990)** and are defined as reversals of the meridional GPH500 gradient. In accordance to **Scherrer et al. (2006)** the one-dimensional **Tibaldi and Molteni (1990**) algorithm is extended to the two dimensions by varying the latitude between 35° and 75° instead of a fixed latitude:

i) GPH500 gradient towards pole: $GPH500G_P = \frac{GPH500_{\varphi+d\varphi} - GPH500_{\varphi}}{d\varphi} < -10 \frac{m}{^{\circ}lat}$ (1)

ii) GPH500 gradient towards equator: $GPH500G_E = \frac{GPH500_{\varphi} - GPH500_{\varphi-d\varphi}}{d\varphi} > 0 \frac{m}{^{\circ}lat}$ (2)

Blocks by definition are persistent and quasi-stationary high-pressure systems that divert or severely slow down the usually prevailing westerly winds in the mid-latitudes. They influence regional temperature and precipitation patterns for an extended period. Therefore, not all blocks that fulfill the two above–mentioned two conditions are retained. We only include blocks that have a minimum required lifetime of 5 days and a minimum overlap of the blocked area of 70% ($A_{t+1} \cap A_t > 0.7 * A_t$) in our blocking catalog. This largely follows the criteria defined by **Schwierz et al. (2004)**.

b) Climate reconstructions

To be as independent as possible with regards to the reanalyses we use a wide array of climate index reconstructions for the 20th century:

- Atlantic Multidecadal Oscillation (AMO): For the AMO index we take October values based on the **Enfield et al. (2003)** study. We choose October to allow for a certain feedback lag with the atmosphere and to have decent prediction value for the upcoming snow and NAO indices.
- El Niño – Southern Oscillation (ENSO): We chose the ENSO3.4 reconstruction based on the HadISSTv1 **Rayner et al. (2003)** SSTs. As with the AMO, we select October values to allow for a reaction time in the teleconnections.

- North Atlantic Oscillation (NAO): We use the extended **Jones et al. (1997)** NAO index for DJF from the Climate Research Unit (CRU).
- Sea Ice: We use the monthly sea ice reconstruction by **Walsh et al. (2017)** which covers the period 1850–2013 to create a Barents-Kara (65–85°N, 30–90°E) sea ice index for November.

We checked for autocorrelation in the time series of the snow indices, stratospheric index, BKS sea ice index (Supplementary Figure 5), AMO index and ENSO index and only found significant autocorrelation in the BKS sea ice and AMO time series. We assess the significance of a regression coefficient in a regression model by dividing the estimated coefficient over the standard deviation of this estimate. For statistical significance we expect the absolute value of the t-ratio to be greater than 2 or the P-value to be less than the significance level (α=0.05). The df are determined as (n-k) where as k we have the parameters of the estimated model and as n the number of observations.

3. Results

a. Interannual links

In the following paragraphs we investigate the year-to-year relationship between the snow indices and the following winter SLP fields. For this we use MERRA2 for a 35-year-long period ranging from 1981–2015, ERA20C for a 110-year-long window ranging from 1901–2010 and 20CRv2c for a 160-year-long window ranging from 1851–2010.

Figure 2 shows the linear regression fields of DJF SLP anomalies projected onto the respective snow indices in October and November. For October, we find no NAO-like pressure anomaly appears to be significantly correlated with the snow index in eacb of the three reanalysis products and respective time windows (Figure 2a,b,c). Instead, negative SLP anomalies dominate Northern Eurasia in MERRA2, with high pressure anomalies towards the Himalayan Plateau. The 110-year-long regression in ERA20C shows significant negative anomalies over the Asian part of Russia, reaching as far south as Beijing. A second significant negative SLP pattern appears along the Pacific coast of Canada. Finally, SLP anomalies in 20CRv2c support the main SLP patterns shown by ERA20C, but reduce the extent of negative

anomalies over Eurasia and increase the extent of the negative anomalies over the North Pacific.

The DJF SLP anomaly patterns change substantially when projected onto the November snow index (Figure 2d,e,f). All three reanalysis products show negative NAO-like pressure anomalies with significantly positive anomalies over Iceland and the northern North Atlantic and significantly negative anomalies south of ca. 45° N, including Portugal and the Azores. As expected, MERRA2 shows the strongest anomalies due to the shorter regression period, however interestingly ERA20C, with the 110-year long analysis period, shows less large-scale significance for positive anomalies in high latitudes compared to the 150-year-long investigation period in 20CRv2c (even though non-significant anomalies cover roughly the same area as in 20CRv2c (not shown)). This hints towards decadal variations in the strength of the regression, but could also be due to biases in the reanalyses.

To check for such biases we compared all reanalyses with the SLP reconstruction dataset HadSLP2r (**Allen and Ansell 2006)**, and found that for the regression analysis using the time period 1901–2010, 20CRv2c overestimates the polar sea level pressure response, whereas ERA20C is much closer to HadSLP2r (See Supplement Figure 6). This would indeed support the notion of decadal variations in the strength of the relationship between predictor and predictand. However, it is worth highlighting that this overestimation for 20CRv2c is not visible for the 1851–2010 period, where the regression anomalies resemble HadSLP2r much closer.

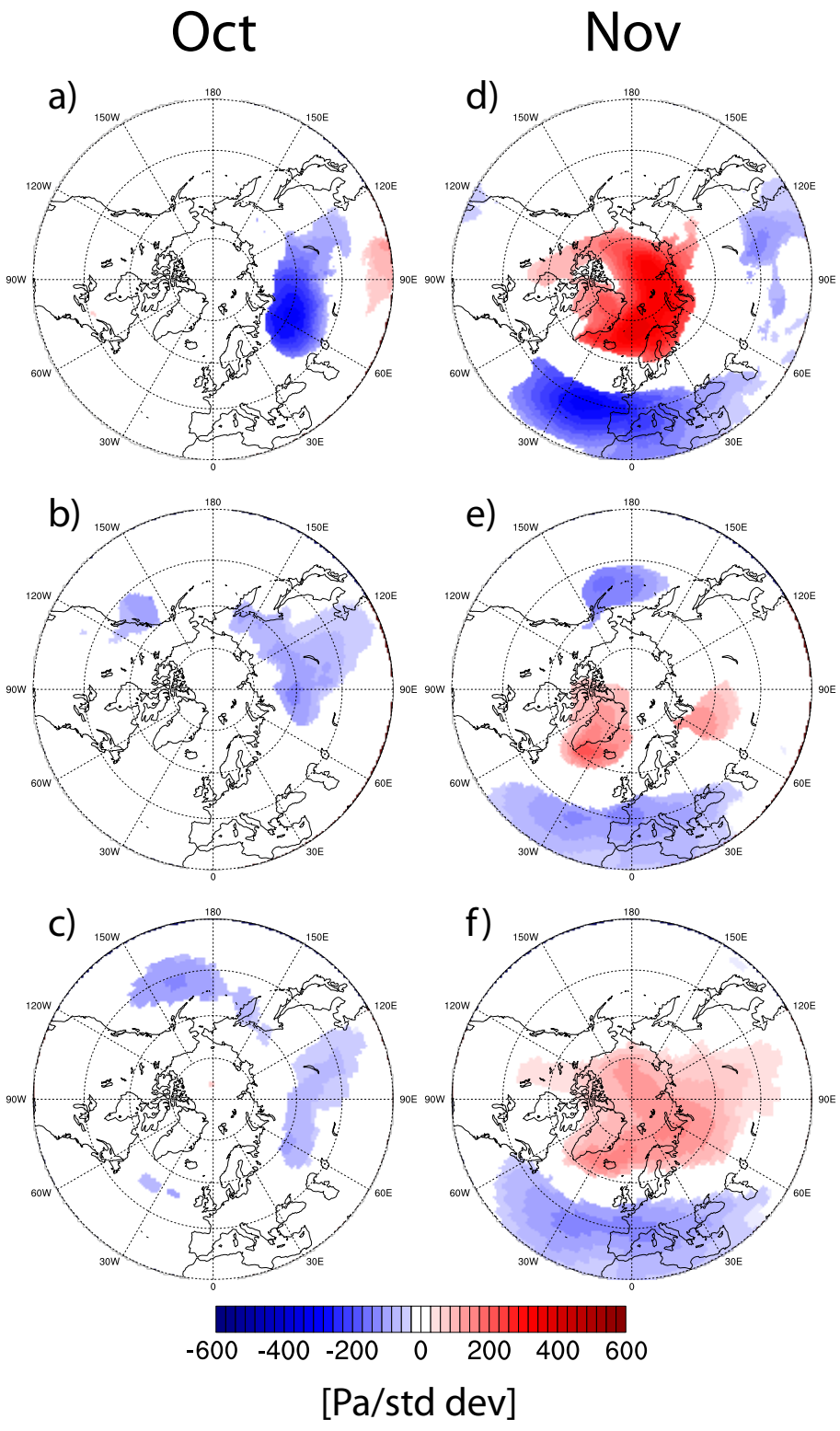

Figure 2: DJF sea level pressure [Pa/std dev] anomalies projected onto snow indices (see Figure 1) for October (left) and November (right) for a and d) MERRA2 covering 1981–2015, b and e) ERA20C covering 1901–2010 and c and f) 20CRv2c covering 1851–2010. Only anomalies >95% significance level are shown.

We investigate other possible predictors for wintertime NAO via regressed anomalies onto the November Barents-Kara-Sea (BKS) ice concentration, November–December mean polar

GPH at 10 hPa, October AMO and October ENSO indices (Figure 3). The periods for MERRA2 and ERA20C are identical as for Figure 2, whereas the anomaly plots for 20CRv2c are using the maximum period covered in the reconstructions, namely 1851–2010 in the sea ice reconstruction, 1856–2010 in the AMO reconstruction, 1901–2010 for the polar 10 hPa GPH index taken from ERA20C, and 1870–2010 for the ENSO reconstruction.

As can be seen from Figure 3, the 35-year-long analysis in MERRA2 shows November sea ice concentration and early winter stratospheric heights to regress a similar SLP pattern than the November snow index. Positive SLP anomalies over Iceland and Greenland combined with negative anomalies over Southern Europe and the adjacent North Atlantic shape a negative NAO-like pattern in DJF (Figure 3a). On the other hand, the interannual signals in the October AMO and ENSO indices do not point towards such a pressure distribution. The small interannual changes and low frequency of the AMO combined with the short sample period prohibit most of the significance, only Southern Eurasia shows regions with elevated SLP. Anomalies regressed on the ENSO index show, as expected, significance mostly for the North Pacific and North American region.

Looking at the regression patterns in the centennial reanalyses, the NAO-like pattern in the SLP anomalies regressed onto sea ice and stratospheric GPH can still be seen, however the extent and strength is substantially reduced compared to MERRA2 as well as compared to the regression using November snow as predictor. Again, ERA20C shows a decrease in the significant anomalies regressed onto sea ice compared to 20CRv2c, with possible reasons already discussed above. Elevated geopotential heights at 10 hPa consistently increase polar sea level pressure in the following winter months, however the impact over the European and North Atlantic domain severely decreases in the centennial reanalyses.

SLP anomalies regressed onto the AMO index show significant positive SLP regions for large parts of Eurasia as well as positive anomalies over the North Atlantic west of Great Britain. Interesting to note in 20CRv2c is the very strong high-pressure anomaly reaching from the BKS to the southern part of the Ural mountains, a prominent feature often found for years with positive AMO and negative sea ice concentration, frequently linked to a high frequency of Ural blockings (UBs). SLP distribution after El Niño events does not change considerably irrespective of the dataset and time period used. A strong Pacific signal shows the northern part of the Pacific-North American pattern (PNA) with negative SLP anomalies over the eastern North Pacific. Given the autocorrelation in the AMO and BKS sea ice index, the

significance in Figure 2abc as well as Figure 2ghi might be severely lower due to the reduced amount of degrees of freedom.

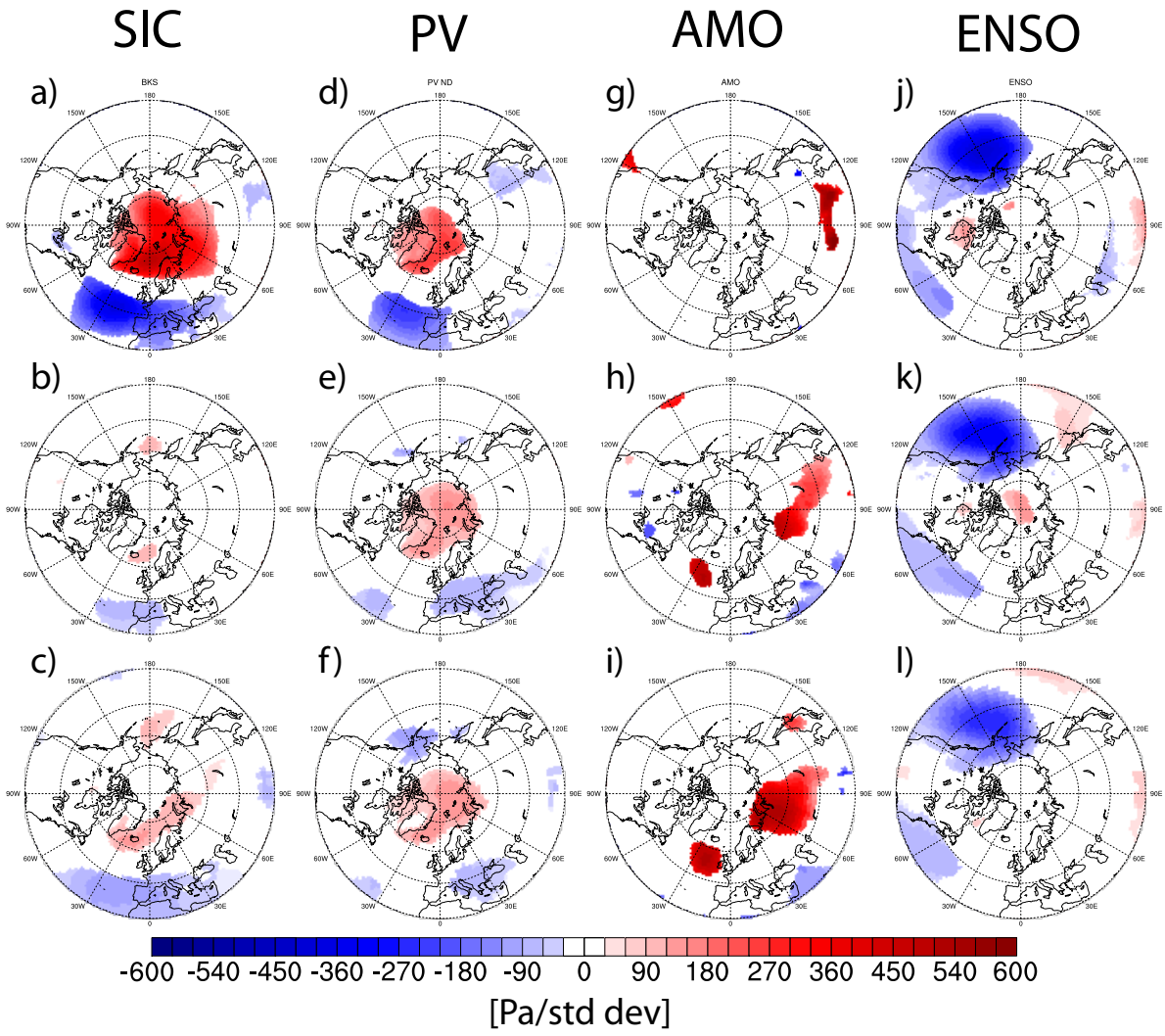

Figure 3: DJF sea level pressure [Pa/std dev] anomalies projected onto BKS ice concentration in November (far left), polar 10 hPa GPH November December mean (left), October AMO (right) and October ENSO indices (far right) for adgj) MERRA2 covering 1981–2015, behk) ERA20C covering 1901–2010 and cfil) 20CRv2c covering 1851–2010. Regression values for BKS ice concentrations were multiplied by minus one to aid comparability. Only anomalies >95% significance level are shown.

To investigate the vertical development of climate anomalies connected with the November snow dipole, Figure 4 shows the zonal mean anomalies of zonal wind and temperature in ERA20C projected onto the ERA20C November snow index (for an evaluation with an upper-air climate reconstruction see Supplementary Figure 7). The temporal evolution of the anomalies ranging from October to February shows that stratospheric warming occurs

simultaneously within the same month as a positive snow cover dipole, with no stratospheric warming leading that development. Instead, significant lower troposphere warming is shown between 60°–90°N for October. The warming signal then dominates the stratosphere and upper troposphere in December, after which the strongest anomalies subside into the lower stratosphere and tropopause in January and February. This development of atmospheric temperatures is mirrored in the evolution of the polar vortex, where a reduction of the polar vortex and strengthening of the subtropical jet is seen together with the emergence of the November snow dipole, after which the region of strongest anomalies migrates from the upper stratosphere to the upper troposphere.

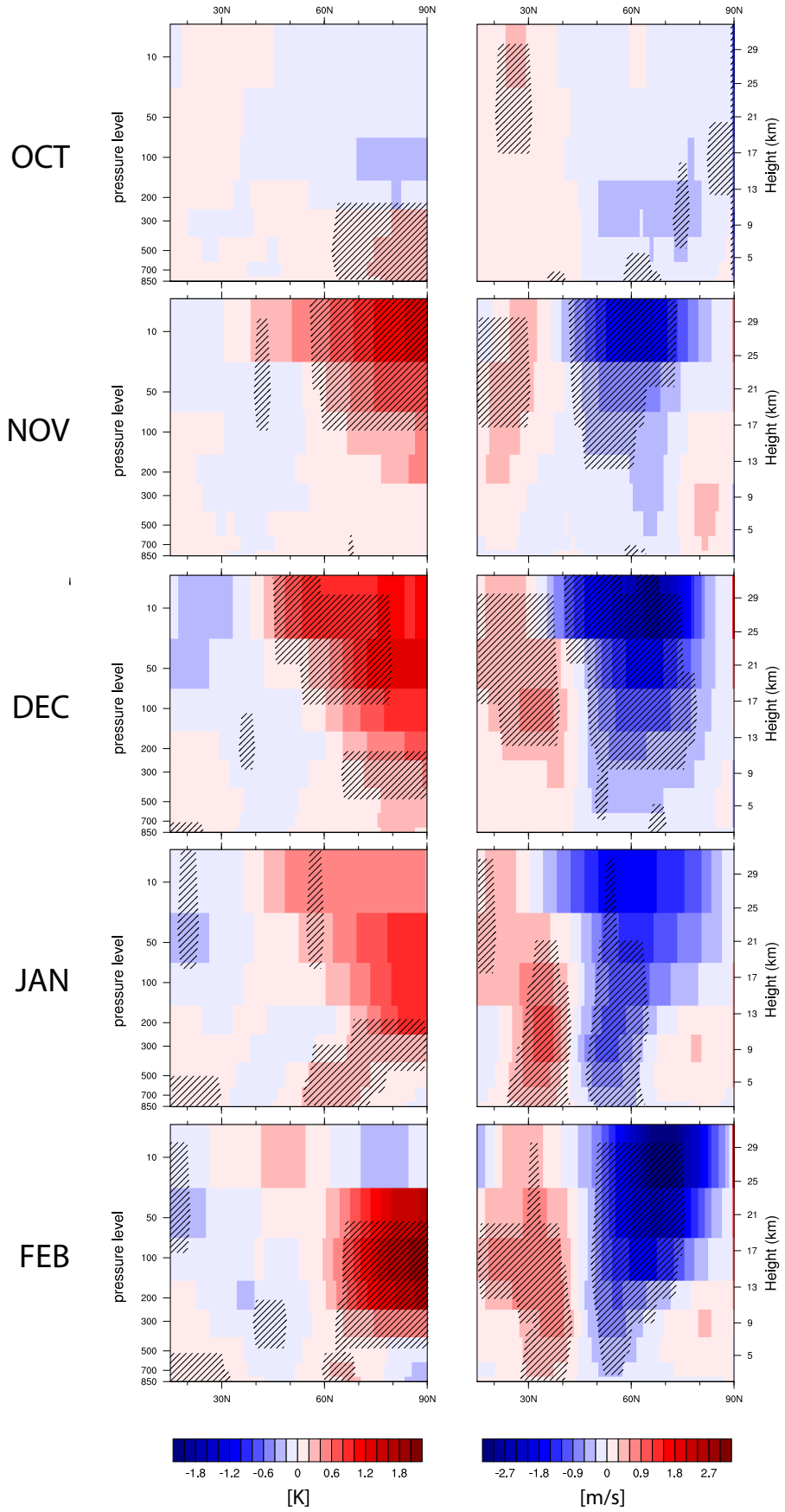

328

329 *Figure 4: Zonal mean (180°E–180°W, 15°N–90°N) left) temperature anomalies and right) zonal mean zonal wind anomalies*
330 *projected onto snow indices in November for ERA20C covering 1901–2010. Shading indicates 95% significance level.*

To address the physical reasons as to how the low sea ice and high snow indices are connected, climate anomalies are regressed onto BKS ice concentrations for November (Figure 5). Compared to factors such as AMO and ENSO, BKS sea ice shows a distinct snow cover dipole coinciding with a high-pressure anomaly over the BKS and the northern Ural mountains, which supports a regional atmospheric blocking and cold air advection on its eastern flank. This cold air anomaly supports increased snow cover over eastern Eurasia, while relatively warm temperatures reduce the snow cover over eastern Europe. It should be noted that October BKS ice concentration shows qualitatively the same pattern for November snow cover anomalies (not shown), however not statistically significant.

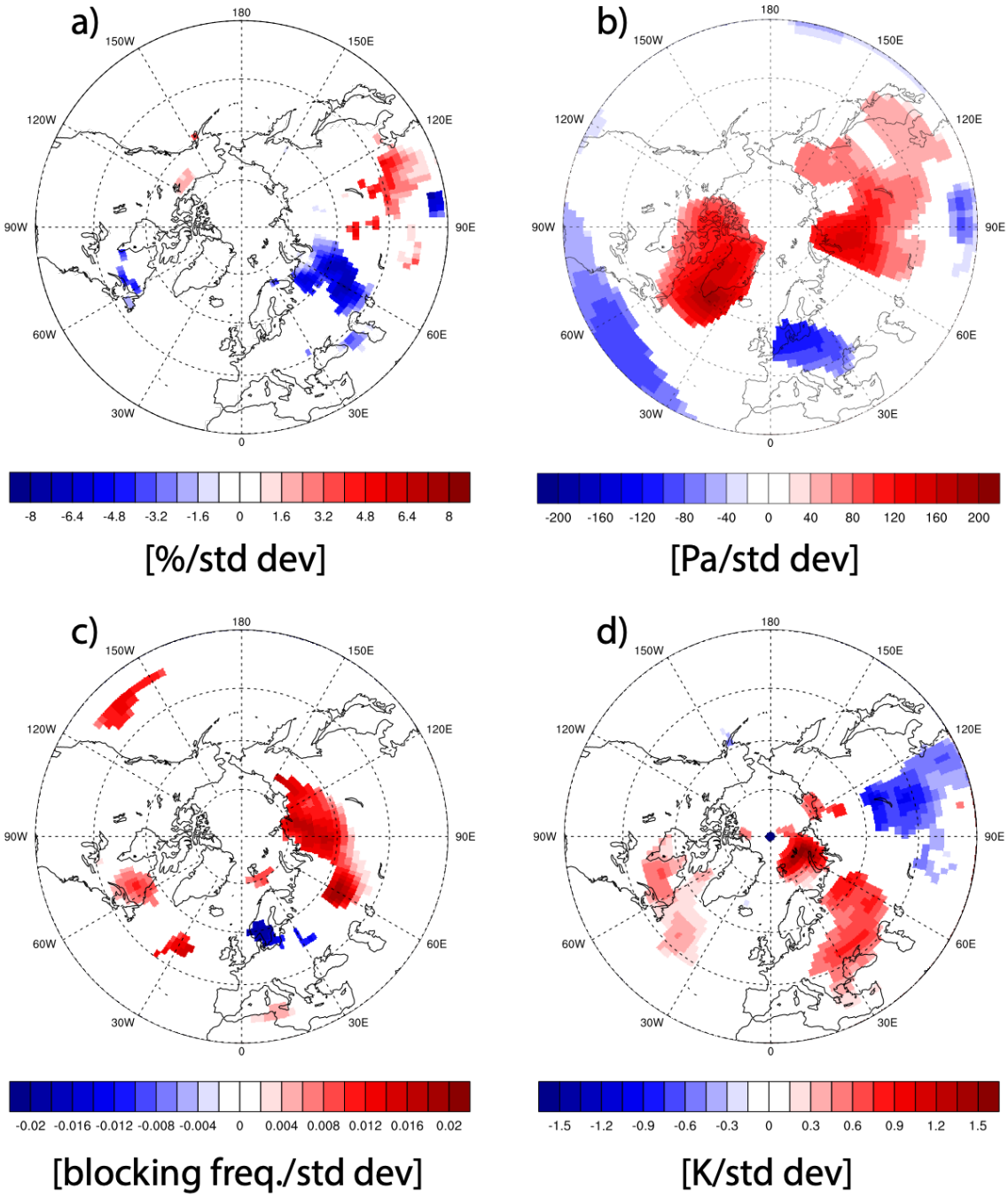

Figure 5: 20CRv2c November anomalies projected onto BKS ice concentration in November covering 1851–2010. Regression values for BKS ice concentrations were multiplied by minus one to aid comparability. a) November snow cover [%/std dev] anomalies projected onto BKS ice concentration in November, b) November SLP [Pa/std dev] anomalies projected onto BKS ice concentration in November, c) November atmospheric blocking [blocking per season/std dev] anomalies projected onto BKS ice concentration in November and d) November 2m temperature [K/std dev] anomalies projected onto BKS ice concentration in November. Only anomalies >95% significance level are shown.

b. Interdecadal links

The interdecadal evolution of the November snow index is shown in Figure 6. 21-year running means of the normalized time series of AMO, BKS ice and snow hint towards a multidecadal frequency, similar in wave length to the AMO and BKS ice anomalies. Even though we refrain from correlating these time series due to the the 21-year filter (**Trenary and DelSole, 2016**), we find the possible mechanism behind the decadal co-occurrence of warm North Atlantic SSTs, reduced sea-ice and increased snow cover gradient to be physically plausible (**Luo et al. 2017**). As **Luo et al. (2017)** point out, warm North Atlantic water reduces the BKS ice concentration, which decreases the meridional temperature gradient and strong westerly winds, which in turn supports high pressure over the Ural mountains and with that, cold air advection towards eastern Eurasia. It should be noted however, that the AMO and the November snow index are out-of-phase between 1880 and 1920, where uncertainties in both products are largest.

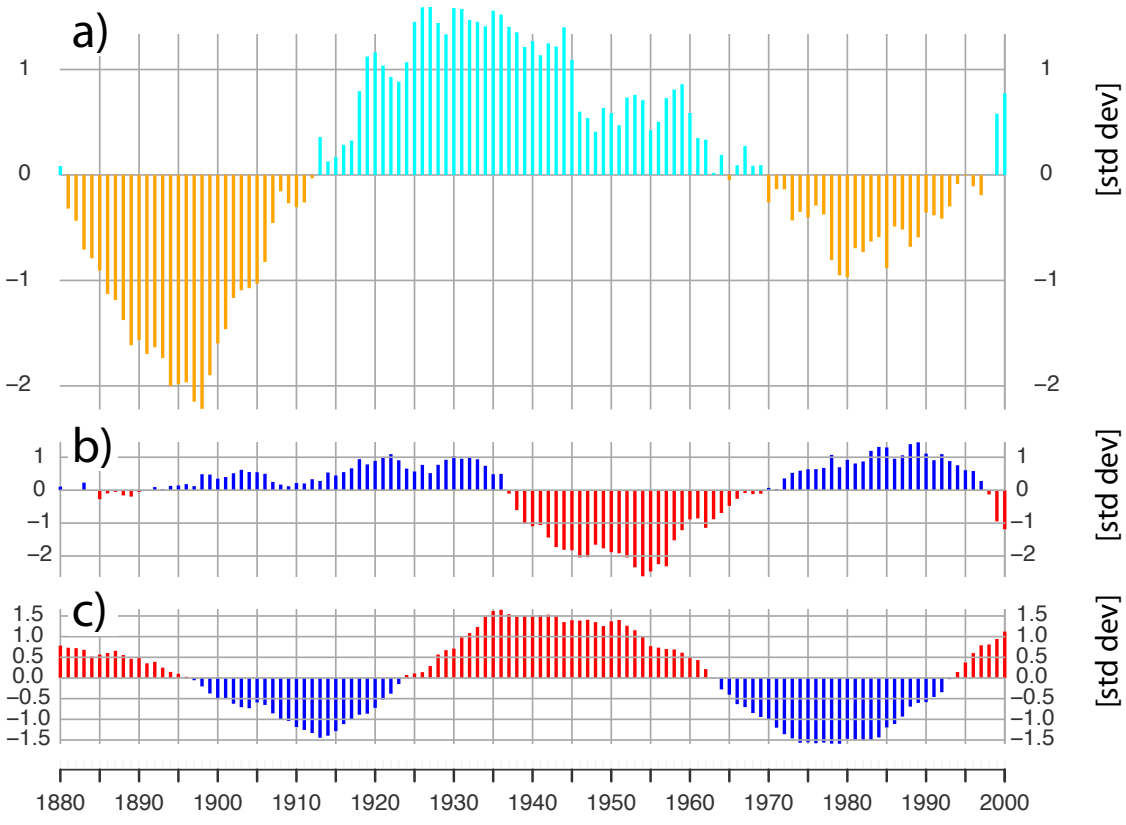

Figure 6: 21-year running means of a) November snow index from 20CRv2c, b) November BKS ice concentration, c) October AMO

The more critical question is the interdecadal evolution of the relationship between the predictor and the predictand. Similar to **Peings et al. (2013)** and **Douville et al. (2017)**, we

apply a 21-year running correlation covering the period 1901–2010 to examine the stationarity of the relationship and differences between 20CRv2c and ERA20C.

Figure 7 summarizes the correlation over time for multiple pairs of climate variables. As Figure 7b points out, the sign of the November snow to winter NAO relationship in 20CRv2c is negative throughout the whole 20th century. Periods with negative correlations can be found at the beginning and the end of the century, with relatively weak correlation during the 1930s and 1970s. The periods of strong negative correlations overlap with commonly known Arctic warming periods, the early 20th-century Arctic warming (ETCAW) and the ongoing recent Arctic warming in context of anthropogenic global warming. In ERA20C, these periods are actually marked by positive correlations, indicating a non-stationary relationship between these two variables. Even stronger decadal variability can be seen for the running correlations between the October snow index and winter NAO-like signal (Figure 7a), with periods of pronounced negative correlations during the early 20th century Arctic warming and the 1980s. Emerging since the 1970s is a negative relationship shown in Figure 7e between BKS ice reduction (multiplied by minus one to aid comparability) and the formation of a negative NAO signal in the following winter, with very weak negative correlations for the ETCAW.

Together with the emergence of the sea ice to NAO relationship, negative correlations between BKS sea ice and November snow index (Figure 7d) as well as between stratospheric warming and winter NAO strengthen towards the end of the 20th century (Figure 7f). This strengthening is also found in ERA20C for the correlation between November snow and a following stratospheric warming, where 20CRv2c shows consistently positive correlation values throughout the 20th century (Figure 7c).

Overall, the 20CRv2c November snow index shows a more stationary relationship with tropospheric and stratospheric winter circulation than ERA20C. Possible explanations for this behavior will be discussed in the following section.

For all of the linear relationships shown in Figure 7 we performed a Durbin-Watson test to check for serial correlation between two variables and did not find any compelling indication for co-dependence in any case (see Supplementary Table 1). Moreover, we investigated different running correlation windows (11 years, 21 years, 25 years, and 31 years) and find that the main outcome of the analysis is not dependent on the choice of the correlation window (see Supplementary Figure 8).

Figure 7: 21-year centered running correlation time series between a) October snow index and DJF NAO, b) November snow index and DJF NAO, c) November snow index and mean November December polar 10 hPa GPH index, d) November snow index and November BKS ice concentration, e) November BKS ice concentration ***multiplied by minus one to aid comparability*** *and DJF NAO and f) mean November December polar 10 hPa GPH and DJF NAO index. Black dashed line indicating the 95% confidence level for a two-sided students T-test assuming independence and normal distribution.*

Based on the results from Figure 7 (and the overall significance of linear relationships, see Supplementary Figure 9) we investigate very basic linear multiple and simple regression

models to predict the upcoming DJF NAO index sign and assess the contributions to the prediction skill by November sea ice, November snow cover and November December mean stratospheric conditions. For the period 1901–2010 we investigate three different multiple regression models with

a) DJF NAO(t) = a1 × Nov. snow cover(t) + b1 × Nov. BKS sea ice(t) + c1 × ND 10hPa GPH(t)

b) DJF NAO (t) = a1 × Nov. snow cover(t) + b1 × Nov. BKS sea ice(t)

c) DJF NAO (t) = a1 × Nov. snow cover(t) + b1 × ND 10hPa GPH(t)

and one simple linear regression model

d) DJF NAO (t) = a1 × Nov. snow cover(t)

where DJF NAO is the standardized NAO index calculated by EOF analysis of 20CRv2c SLP data, Nov. snow cover is the November 20CRv2c snow cover index, Nov. BKS sea ice is the Walsh et al. November BKS sea ice index and ND 10hPa GPH is the ERA20C November December mean 10hPa GPH index with a1,b1,c1 being the constants determined by the least-squares calculations. Moreover, we perform b) and d) also for the period 1851–2010.

Figure 8 shows original and predicted normalized DJF NAO values together with the 21-year running correlation of both indices. Overall correlation values are low but significant for the 110-year time period (ranging from 0.41 to 0.38) but specific periods of high correlation emerge for both Arctic warm periods, the first one being centered around 1925 and the second one being centered around the year 2000 with both periods reaching correlation coefficients above 0.6. The multiple regression prediction model with three different predictors performs best, with a significant correlation to the original NAO variability of 0.41 for 110 years (Figure 8a). Nevertheless, November snow cover seems to add most of the prediction skill, since the decrease in correlation coefficient between the multiple regression model with three predictors and the simple linear regression model with just November snow cover as a predictor is 0.03. Moreover, periods of high correlation coefficients align with periods of strong negative relationships in Figure 7b.

For the same empirical prediction model using 160 years, the overall correlation coefficients decrease to around 0.3. As expected, the same periods of increased prediction skill emerge

(Figure 8e&f) and the added prediction skill of sea ice is low. It should be noted however, that sea ice increases prediction skill during the current Arctic warming period, as well as the end of the 19th century with 2nd highest correlation coefficients centered around 1890 (not shown).

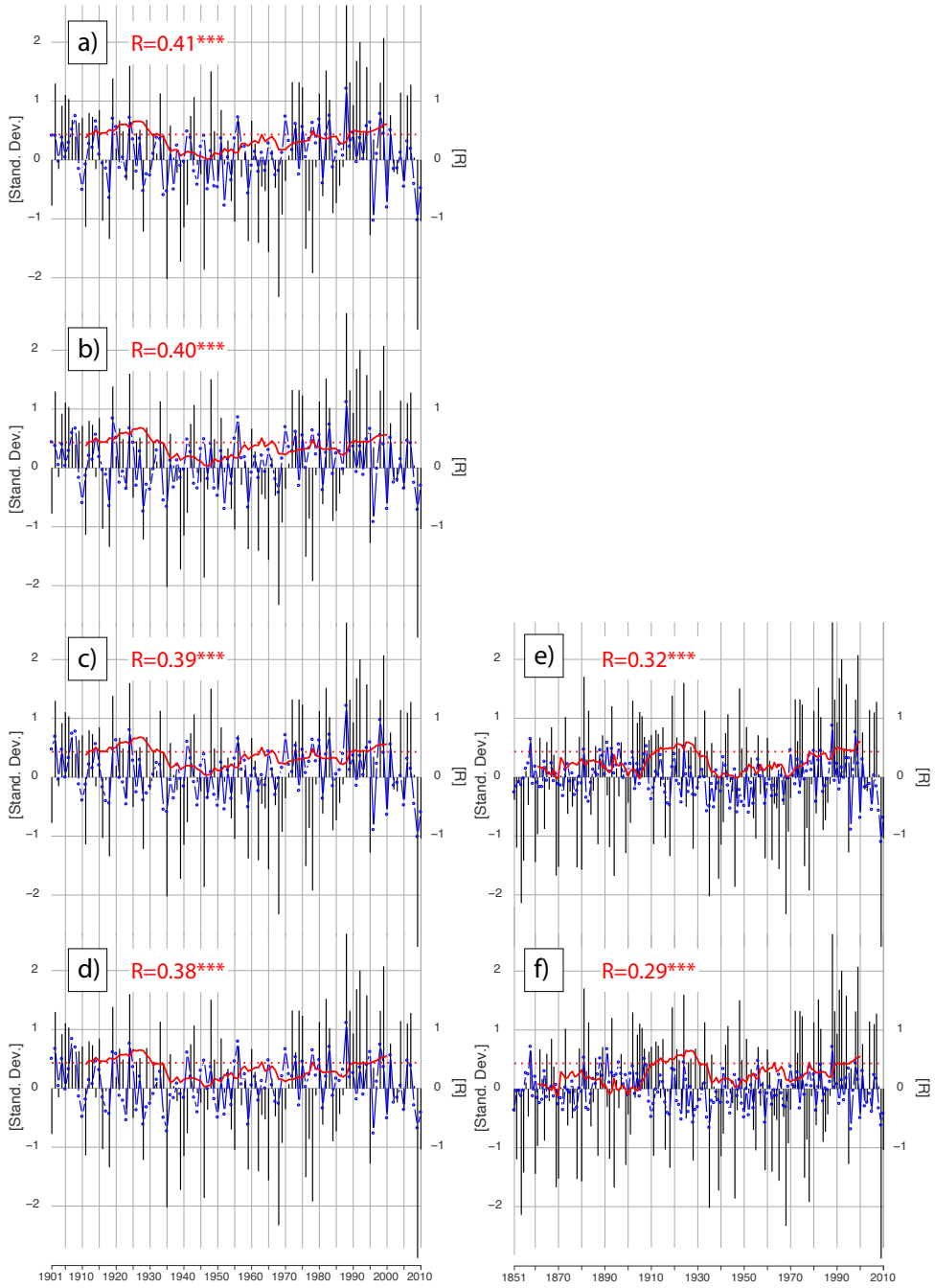

Figure 8: Comparison of 1901–2010 20CRv2c DJF standardized NAO values based on EOF analysis with predicted values from multiple and simple linear regression models showing a) multiple linear regression model with November snow cover index, November BKS sea ice index and ND 10hPa geopotential height index with an overall correlation of 0.41, b) multiple linear regression model with November snow cover index and ND 10hPa geopotential height index with an overall correlation of 0.4, c) multiple linear regression model with November snow cover index and November BKS sea ice index with an overall correlation of 0.39, d) simple linear regression model with November snow cover index and November BKS

sea ice index with an overall correlation of 0.38. e) and f) same as c) and d) but for the period 1851–2010 respectively. Left Y-axis indicates standard deviation, right Y-axis indicates correlation coefficient. Red dashed line indicates 95% significance level for a 21-year period.

4. Discussion

We used a variety of reanalyses and reconstructions to address some of the open questions regarding the relationship between Eurasian snowe cover and the state of the NAO in the following winter.

Given the highly discussed research topic of Northern Hemisphere sea ice cover and snow cover impact on mid-latitude circulation **(Cohen et al., 2019),** as well as the highlighted need to investigate relationships over several decades (**Kolstad and Screen 2019**), we investigated a promising November west-east snow cover dipole over Eurasia (**Gastineau et al., (2017); Han and Sun (2018))** and its relationship to the DJF NAO state up to the middle of the 19th century to cover 150 years of internal and external climate forcings. Given the importance for seasonal prediction, we addressed the question of stationarity of said relationship as well as its context within other common Northern Hemispheric predictors.

Compared to **Gastineau et al. (2017) and Han and Sun (2018),** we could extend the reanalysis study period from 35 to 150 years and highlighted the consistently negative sign of the snow-NAO relationship in the 20CRv2c dataset. Partial correlations for 110 years show that reduced BKS sea ice shows a similar response in DJF SLP anomalies, however its statistical importance, and therefore quality as being the prime predictor, is less than the November snow index (see Supplementary Table 2 for partial correlations). This is also found in simple multiple regression prediction models, where the November snow cover index was incorporating the major share of the prediction power. Extending the analysis of **Gastineau et al. (2017)** to 150 years further underlines the lack of snow–atmosphere feedback in most of the CMIP5 models and reduces the probability that the snow-NAO link is due to random internal variability at the end of the 20th century.

Moreover, given the monthly development of vertical temperature anomalies related to a high snow cover index supports the theoretical framework (**Cohen et al., 2014; Henderson et al. 2018**) for a Eurasian snow cover to stratosphere link in reanalyses for at least the 20th century and probably beyond. We found surface cooling and snow cover expansion east of the sea ice

anomaly, where cold air is advected on the eastern side of a Ural blocking anomaly (Figure 5). The increased geopotential heights and the related Rossby-Wave energy reach the stratosphere (Supplementary Figure 7), where a stratospheric warming and a slow down of the Polar Vortex manifests (Figure 4). These anomalies reach the troposphere in January and February where they express themselves as a negative NAO signal (Figure 2). It is noteworthy, that all of these features are significantly correlated with the November snow cover index for more than 100 years.

Peings et al. (2013) and the follow up study by **Douville et al. (2017)** found that the October and October–November mean snow cover over a broader region of Northern Eurasia, and its relationship to the wintertime NAO is indeed not stationary over time. We found a strong relationship between the reduced variance of the snow index time series with the reduction in correlation strength of snow cover and the wintertime NAO (Figure 9). The reduction of variance is even stronger in ERA20C than in 20CRv2c, which would explain the less stationary correlations in ERA20C. Furthermore, such periods of low snow variability coincide with a reduction of polar vortex variability, hinting even more so towards possible links between November snow and stratospheric temperatures in the following month. Together with the snow cover index, the November BKS sea ice index shows increased variability with strengthened negative correlation to DJF NAO during at the end of the 20th century (see Supplementary Figure 11).

These periods of increased variability in the November snow cover index co-occur arguably with the common Arctic warming periods of the 20th century, the ETCAW (**Wegmann et al., 2016; Hegerl et al., 2018**) and the recent ongoing Arctic warming with peak variance and correlation values centered around the years 1920 and 2000. Interestingly, October snow cover index and BKS sea ice index variability peaks slightly after the ETCAW around the year 1945. Analysing temperature anomalies (not shown) for all three periods reveals more continental warming over Russia for the period 1911-1930 whereas warming between 1936-1955 is located very much at the Kara Sea coast of Russia. Both, the October snow index and the BKS sea ice index, are thus impacted by the locally increased near-surface temperatures during the latter period. Generally, Arctic warming periods appear to increase variability of cryospheric predictors considerably and thus strengthen their value in seasonal prediction frameworks. Given the importance of stratospheric variability for seasonal prediction and the apparent relationship between snow cover variability and stratospheric variability (Figure 9), it can be expected that the cryosphere-stratosphere pathway is also considerably stronger in

Arctic warm periods than for cold periods. Moreover, in our statistical analysis, we found no indication for a stratospheric precursor of November snow cover anomalies.

In accordance to the shorter time frame analysis of **Sun et al. (2019)**, decadal variability of the November snow cover index seems mostly dominated by low-frequency variability in the AMO and subsequently reduced or increased polar sea ice concentration. This mechanism is also supported by the results of **Luo et al. (2017)**, who highlighted the decadal relationship between a positive AMO, reduced sea ice and increased Ural blocking for the second half of the 20th century. Looking at this mechanism on an interannual basis, we showed a robust strengthening of the November snow dipole with decreasing BKS ice concentration, circulation changes over the BKS region and consequently cold air advection towards the eastern part of the snow dipole region for a period of 150 years. With this, our results support recent studies, which point out the counterintuitive mechanism of Arctic warming and increased continental snow cover via sea ice reduction and circulation changes (**Cohen et al., 2014; Wegmann et al., 2015; Yeo et al., 2016; Gastineau et al., 2017**).

Peings (2019) performed model experiments with nudged November Ural blocking fields, BKS ice and snow anomalies. The author found that UB events are not triggered by reduced sea ice, but in fact lead sea ice decrease. Moreover, more November snow alone did not lead to an increase in blocking frequency, nor to a stratospheric warming. The study highlights the UB events as primary predictor for a negative NAO and the Warm Arctic-cold Continents (WACC) pattern. On the other hand, **Luo et al. (2019)** established a causal chain via a stratospheric pathway from reduced sea ice to reduced potential vorticity gradient and increased blocking events leading to cold extremes over Eurasia. We computed the field average of blocking frequency within the domain of **Peings (2019)** (10°W-80°E, 45-80°N) and could find a strong correlation with the WACC pattern over time, however only for DJF blocking events (not shown).

We found a correlation of November UB events with wintertime NAO, which however is still weaker than the relationship with the November snow dipole, as well as our BKS ice index (see Supplementary Figure 10). Moreover, blockings within the domain of **Peings (2019)** (10°W-80°E, 45-80°N) are not related to a snow dipole whatsoever, neither in October nor in November (see Supplementary Figure 10). That said, we want to highlight the fact that the blocking pattern emerging in Figure 5 is mostly outside of the boundaries of this UB index (10°W-80°E, 45-80°N), and thus might not be caught by this recent study. Furthermore, **Peings (2019)** applies a very general snow cover increase in his nudging experiment, rather

than a snow dipole with a west to east gradient. Finally, although we focused here on the connection to the NAO, we did not find strong significant correlations between autumn snow and winter WACC. As pointed out by **Peings (2019)**, the most important driver for the WACC signal is the Ural blocking, for which we found strong correlations throughout the 20th century (not shown).

Overall, we advocate the importance of the signal-to-noise ratio rather than mean states for the evolution of the November snow to winter NAO relationship. In our statistical analysis, we did not find any indication for a centennial relationship between the autumn ENSO or autumn QBO sign with the variability of the relationship between November snow cover and DJF NAO (not shown). As mentioned above we found the strongest influence to be the increased variability of the system due to energy uptake.

That said, a source of uncertainty is the disagreement between ERA20C and 20CRv2c when it comes to the stationarity of the relationship. 20CRv2c shows negative correlation throughout the whole 20th century, whereas ERA20C flips the sign of the correlation in the late 1930s and late 1970s. The same relationship but using October snow shows high agreement between the two datasets, which is the same case for the correlations between snow and stratospheric GPH. We therefore conclude, that the information stored in the November snow cover in 20CRv2c is slightly different to the information stored in the ERA20C snow depth. **Wegmann et al. (2017**) found that Eurasian November snow depth shows much larger disagreement between 20CRv2c and ERA20C than the same snow depth in October. In the same study, the authors found decadal trends (although linear trend subtraction for all predictor time series was done for this study) in ERA20C snow depth which might impact the running correlations. Finally, since snow depths are relatively low in October, differences between using snow cover and snow depth might be less important from an energy transfer point of view.

The disagreement between ERA20C and 20CRv2c may also be related to uncertainties and inhomogeneities in both reanalyses. Many studies showed that both ERA20C and 20CRv2c are not suitable for studies looking at trends (e.g. **Brönnimann et al., 2012; Krüger et al., 2013**) and may include radical shifts in atmospheric circulation, particularly over the Arctic (e.g. **Dell'Aquila et al., 2016; Rohrer et al., 2019**). However, **Rohrer et al. (2019)** showed that although trends in centennial reanalyses may be spurious, at least in the Northern Hemisphere year-to-year variability of mid-tropospheric circulation is in agreement even in the early 20th century.

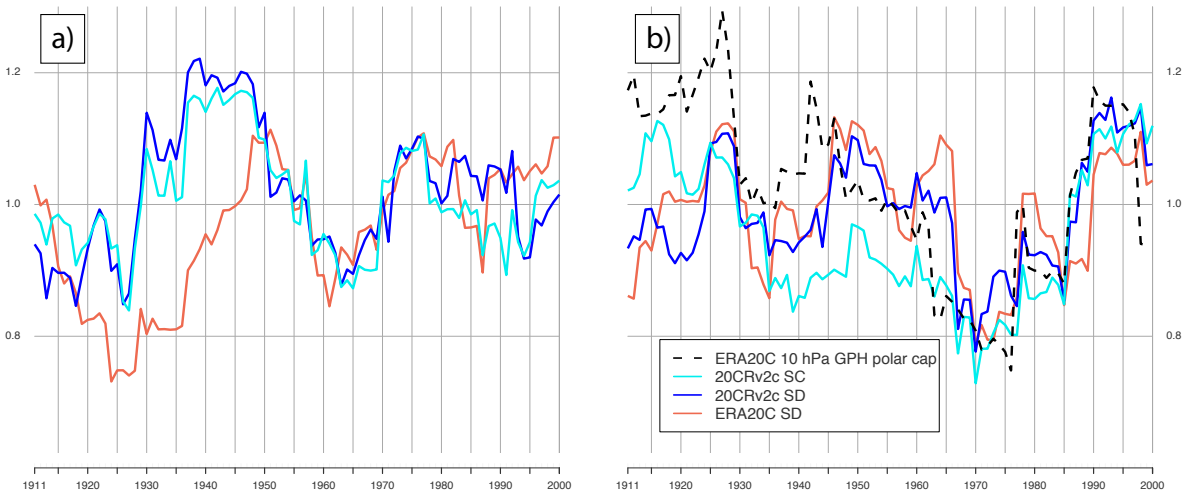

577

578 *Figure 9: 21-year running standard deviation time series of a) October snow index and b) November snow index in ERA20C*
579 *and 20CRv2c (snow cover and snow depth). Dashed black line shows running standard deviation of 10 hPa November*
580 *December mean GPH over the polar regions.*

581 ## 5. Conclusion

582 Several reconstruction and reanalysis datasets were used to examine the link between autumn
583 snow cover, ocean surface conditions and the NAO pattern in winter for the whole 20th
584 century and into the 19th century. We found evidence for a manifestation of a negative NAO
585 signal after November with a strong west-to-east snow cover gradient, with this relationship
586 being significant for the last 150 years. Interdecadal variability for this relationship seems to
587 be linked to Arctic warm periods which increase the variability of the cryospheric predictors
588 considerably. As a result, increased variability in the predictors helps to generate a better
589 seasonal prediction estimation.

590 Furthermore, our analysis of centennial time series supports studies pointing out the link of
591 autumn snow to stratospheric circulation as well as the co-occurence between reduced BKS
592 ice concentration and increased snow cover in eastern Eurasia. The latter mechanism is
593 triggered via the development of an atmospheric high-pressure anomaly adjacent to the BKS
594 sea ice anomaly, which transports moisture and cold air along its eastern flank into the
595 continent. The interdecadal evolution of the November snow index also points towards co-
596 dependence with high North Atlantic SSTs subsequently reduced sea ice.

597 Extending the investigation period from 35 to 110 and up to 150 years increases the
598 confidence in recently proposed physical mechanisms behind cryospheric drivers of
599 atmospheric variability and decreases the probability of random co-variability between the
600 Arctic cryosphere changes and mid-latitude climate.

For future studies regarding seasonal prediction, we emphasize the use of the November snow dipole concerning a forecasting of the winter NAO state. Nevertheless, periods of weak correlation might occur again, especially since it is uncertain how the sea ice to snow relationship will change with stronger anthropogenic global warming, once the Arctic is ice free in summer or the local warming is strong enough to override the counterintuitive snow cover increase. Thus, further studies are needed to investigate the interplay between Arctic sea ice and continental snow distribution. Future experiments should take into account year-to-year variability and realistic distribution of snow cover if links to the stratosphere are to be examined.

Acknowledgements

Marco Rohrer was supported by the Swiss National Science Foundation under Grant 143219. The Twentieth Century Reanalysis Project datasets are supported by the U.S. Department of Energy, Office of Science Innovative and Novel Computational Impact on Theory and Experiment (DOE INCITE) program, and Office of Biological and Environmental Research (BER), and by the National Oceanic and Atmospheric Administration Climate Program Office. The ECMWF 20th Century Reanalyses and model simulations are supported by the EU FP7 project ERA-CLIM2. We thank Morgan Gray for editorial support.

Data Availability

The MERRA2 reanalysis data is publicly available at the NASA EARTHDATA repository (https://disc.gsfc.nasa.gov/daac-bin/FTPSubset2.pl). The ERA-20C reanalysis data is publicly available at the ECMWF data repository (https://apps.ecmwf.int/datasets/). The 20CRv2c reanalysis data is publicly available at the NOAA Earth System Research Laboratory repository (https://www.esrl.noaa.gov/psd/data/gridded/data.20thC_ReanV2c.html). The blocking algorithm is publicly available at https://github.com/marco-rohrer/TM2D. The AMO reconstruction data is a publicly vailable at the NOAA Earth System Research Laboratory (https://www.esrl.noaa.gov/psd/data/timeseries/AMO/). The Niño 3.4 reconstruction is publicly available at the GCOS Working Group on Surface Pressure repository (https://www.esrl.noaa.gov/psd/gcos_wgsp/Timeseries/Nino34/). The NAO reconstruction is publicly available at the Climate Research Unit repository (https://crudata.uea.ac.uk/cru/data/nao/). The Walsh et al. sea ice concentration reconstruction

632 is publicly available at the National Snow and Ice Data Center repository
633 (https://nsidc.org/data/g10010).

634 **Author Contribution**

635 M.W. devised the study, the main conceptual ideas and the proof outline. M.R. assisted with
636 data availability and performed the blocking algorithm. M.W. wrote the manuscript in
637 consultation with M.S-O. and G.L., who aided in interpreting the results.

638 **Competing interest**

639 The authors declare that they have no conflict of interest.

640 **References**

641 Allan, R., and T. Ansell, 2006: A New Globally Complete Monthly Historical Gridded Mean
642 Sea Level Pressure Dataset (HadSLP2): 1850-2004. J. Climate, 19, 5816-5842.

643 Athanasiadis, P. J., Bellucci, A., Scaife, A. A., Hermanson, L., Materia, S., Sanna, A., ... and
644 Gualdi, S. (2017). A multisystem view of wintertime NAO seasonal
645 predictions. *Journal of Climate*, *30*(4), 1461-1475.

646 Belleflamme A, Fettweis X, Erpicum M (2015) Recent summer Arctic atmospheric
647 circulation anomalies in a historical perspective. Cryosphere 9:53–64

648 Blackport, Russell, and James A. Screen. "Influence of Arctic Sea Ice Loss in Autumn
649 Compared to That in Winter on the Atmospheric Circulation." *Geophysical Research*
650 *Letters* 46.4 (2019): 2213-2221.

651 Blackport, R., Screen, J.A., van der Weil, K., and Bintanja, R. (2019). Minimal influence of
652 reduced Arctic sea ice on coincident cold winters in mid-latitudes. *Nature Climate*
653 *Change*, ?

654 Boland, E. J., Bracegirdle, T. J., and Shuckburgh, E. F. (2017). Assessment of sea ice-
655 atmosphere links in CMIP5 models. *Climate Dynamics*, *49*(1-2), 683-702.

656 Brönnimann, S., Luterbacher, J., Staehelin, J., Svendby, T. M., Hansen, G., and Svenøe, T.
657 (2004). Extreme climate of the global troposphere and stratosphere in 1940–42 related
658 to El Niño. *Nature*, *431*(7011), 971.

659 Brönnimann, S., Xoplaki, E., Casty, C., Pauling, A., and Luterbacher, J. (2007). ENSO
660 influence on Europe during the last centuries. *Climate Dynamics*, *28*(2-3), 181-197.

661 Cohen, J., and Entekhabi, D. (1999). Eurasian snow cover variability and Northern
662 Hemisphere climate predictability. *Geophysical Research Letters*, *26*(3), 345-348.

663 Cohen, J., Barlow, M., Kushner, P. J., and Saito, K. (2007). Stratosphere–troposphere
664 coupling and links with Eurasian land surface variability. *Journal of Climate*, *20*(21),
665 5335-5343.

666 Cohen, J., Screen, J. A., Furtado, J. C., Barlow, M., Whittleston, D., Coumou, D., ... and
667 Jones, J. (2014). Recent Arctic amplification and extreme mid-latitude weather. *Nature*
668 *geoscience*, *7*(9), 627.

669 Cohen, J. (2016). An observational analysis: Tropical relative to Arctic influence on
670 midlatitude weather in the era of Arctic amplification. *Geophysical Research*
671 *Letters*, *43*(10), 5287-5294.

672 Cohen, J., Pfeiffer, K., and Francis, J. A. (2018). Warm Arctic episodes linked with increased
673 frequency of extreme winter weather in the United States. *Nature communications*, *9*(1),
674 869.

675 Cohen, J., Zhang, X., Francis, J., Jung, T., Kwok, R., Overland, J., ... and Feldstein, S. (2019).
676 Divergent consensuses on Arctic amplification influence on midlatitude severe winter
677 weather. *Nature Climate Change*, 1-10.

678 Collow, T. W., Wang, W., Kumar, A., and Zhang, J. (2017). How well can the observed
679 Arctic sea ice summer retreat and winter advance be represented in the NCEP Climate
680 Forecast System version 2?. *Climate Dynamics*, *49*(5-6), 1651-1663.

681 Cram, T. A., Compo, G. P., Yin, X., Allan, R. J., McColl, C., Vose, R. S., ... and
682 Bessemoulin, P. (2015). The international surface pressure databank version
683 2. *Geoscience Data Journal*, *2*(1), 31-46.

684 Crasemann, B., Handorf, D., Jaiser, R., Dethloff, K., Nakamura, T., Ukita, J., and Yamazaki,
685 K. (2017). Can preferred atmospheric circulation patterns over the North-Atlantic-
686 Eurasian region be associated with arctic sea ice loss?. *Polar Science*, *14*, 9-20.

687 Dell'Aquila, A., Corti, S., Weisheimer, A., Hersbach, H., Peubey, C., Poli, P., ... and
688 Simmons, A. (2016). Benchmarking Northern Hemisphere midlatitude atmospheric

689 synoptic variability in centennial reanalysis and numerical simulations. *Geophysical*
690 *Research Letters*, *43*(10), 5442-5449.

691 Deser, C., Hurrell, J. W., and Phillips, A. S. (2017). The role of the North Atlantic
692 Oscillation in European climate projections. *Climate dynamics*, *49*(9-10), 3141-3157

693 Domeisen, D. I., Garfinkel, C. I., and Butler, A. H. (2019). The teleconnection of El Niño
694 Southern Oscillation to the stratosphere. *Reviews of Geophysics*.

695 Douville, H., Peings, Y., and Saint-Martin, D. (2017). Snow-(N) AO relationship revisited
696 over the whole twentieth century. *Geophysical Research Letters*, *44*(1), 569-577.

697 Dunstone, N., Smith, D., Scaife, A., Hermanson, L., Eade, R., Robinson, N., ... and Knight, J.
698 (2016). Skilful predictions of the winter North Atlantic Oscillation one year
699 ahead. *Nature Geoscience*, *9*(11), 809.

700 Enfield, D. B., Mestas-Nuñez, A. M., and Trimble, P. J. (2001). The Atlantic multidecadal
701 oscillation and its relation to rainfall and river flows in the continental US. *Geophysical*
702 *Research Letters*, *28*(10), 2077-2080.

703 Francis, J. A. (2017). Why are Arctic linkages to extreme weather still up in the air?. *Bulletin*
704 *of the American Meteorological Society*, *98*(12), 2551-2557.

705 Furtado, J. C., Cohen, J. L., Butler, A. H., Riddle, E. E., and Kumar, A. (2015). Eurasian
706 snow cover variability and links to winter climate in the CMIP5 models. *Climate*
707 *dynamics*, *45*(9-10), 2591-2605.

708 Furtado, J. C., Cohen, J. L., and Tziperman, E. (2016). The combined influences of autumnal
709 snow and sea ice on Northern Hemisphere winters. *Geophysical Research*
710 *Letters*, *43*(7), 3478-3485.

711 García-Serrano, J., Frankignoul, C., Gastineau, G., and De La Càmara, A. (2015). On the
712 predictability of the winter Euro-Atlantic climate: lagged influence of autumn Arctic sea
713 ice. *Journal of Climate*, *28*(13), 5195-5216.

714 Garfinkel, C. I., Schwartz, C., Domeisen, D. I., Son, S. W., Butler, A. H., and White, I. P.
715 (2018). Extratropical Atmospheric Predictability From the Quasi-Biennial Oscillation in
716 Subseasonal Forecast Models. *Journal of Geophysical Research: Atmospheres*, *123*(15),
717 7855-7866.

718 Gastineau, G., García-Serrano, J., and Frankignoul, C. (2017). The influence of autumnal
719 Eurasian snow cover on climate and its link with Arctic sea ice cover. *Journal of*
720 *Climate*, *30*(19), 7599-7619.

721 Gelaro, R., McCarty, W., Suárez, M. J., Todling, R., Molod, A., Takacs, L., ... and Wargan,
722 K. (2017). The modern-era retrospective analysis for research and applications, version
723 2 (MERRA-2). *Journal of Climate*, *30*(14), 5419-5454.

724 Ghatak, D., Frei, A., Gong, G., Stroeve, J., and Robinson, D. (2010). On the emergence of an
725 Arctic amplification signal in terrestrial Arctic snow extent. *Journal of Geophysical*
726 *Research: Atmospheres*, *115*(D24).

727 Han, S., and Sun, J. (2018). Impacts of Autumnal Eurasian Snow Cover on Predominant
728 Modes of Boreal Winter Surface Air Temperature Over Eurasia. *Journal of Geophysical*
729 *Research: Atmospheres*, *123*(18), 10-076.

730 Handorf, D., Jaiser, R., Dethloff, K., Rinke, A., and Cohen, J. (2015). Impacts of Arctic sea
731 ice and continental snow cover changes on atmospheric winter
732 teleconnections. *Geophysical Research Letters*, *42*(7), 2367-2377.

733 Hegerl, G. C., Brönnimann, S., Schurer, A., and Cowan, T. (2018). The early 20th century
734 warming: anomalies, causes, and consequences. *Wiley Interdisciplinary Reviews:*
735 *Climate Change*, *9*(4), e522.

736 Henderson, G. R., Peings, Y., Furtado, J. C., and Kushner, P. J. (2018). Snow–atmosphere
737 coupling in the Northern Hemisphere. *Nature Climate Change*, 1.

738 Honda, M., Inoue, J., and Yamane, S. (2009). Influence of low Arctic sea-ice minima on
739 anomalously cold Eurasian winters. *Geophysical Research Letters*, *36*(8).

740 Hoshi, K., Ukita, J., Honda, M., Nakamura, T., Yamazaki, K., Miyoshi, Y., and Jaiser, R.
741 (2019). Weak Stratospheric Polar Vortex Events Modulated by the Arctic Sea-Ice
742 Loss. *Journal of Geophysical Research: Atmospheres*, *124*(2), 858-869.

743 Hurrell, J. W., and Deser, C. (2010). North Atlantic climate variability: the role of the North
744 Atlantic Oscillation. *Journal of Marine Systems*, *79*(3-4), 231-244.

745 Inoue, J., Hori, M. E., and Takaya, K. (2012). The role of Barents Sea ice in the wintertime
746 cyclone track and emergence of a warm-Arctic cold-Siberian anomaly. *Journal of*
747 *Climate*, *25*(7), 2561-2568.

748 Jones, P. D., Jonsson, T., and Wheeler, D. (1997). Extension to the North Atlantic Oscillation
749 using early instrumental pressure observations from Gibraltar and south-west
750 Iceland. *International Journal of climatology*, *17*(13), 1433-1450.

751 Jung, T., Vitart, F., Ferranti, L., and Morcrette, J. J. (2011). Origin and predictability of the
752 extreme negative NAO winter of 2009/10. *Geophysical Research Letters*, *38*(7).

753 Kang, D., Lee, M. I., Im, J., Kim, D., Kim, H. M., Kang, H. S., ... and MacLachlan, C. (2014).
754 Prediction of the Arctic Oscillation in boreal winter by dynamical seasonal forecasting
755 systems. *Geophysical Research Letters*, *41*(10), 3577-3585.

756 Kang, W., and Tziperman, E. (2017). More frequent sudden stratospheric warming events due
757 to enhanced MJO forcing expected in a warmer climate. *Journal of Climate*, *30*(21),
758 8727-8743.

759 Kelleher, M., and Screen, J. (2018). Atmospheric precursors of and response to anomalous
760 Arctic sea ice in CMIP5 models. *Advances in Atmospheric Sciences*, *35*(1), 27-37.

761 King, M. P., Hell, M., and Keenlyside, N. (2016). Investigation of the atmospheric
762 mechanisms related to the autumn sea ice and winter circulation link in the Northern
763 Hemisphere. *Climate dynamics*, *46*(3-4), 1185-1195.

764 Kolstad, E. W., and Screen, J. A. (2019). Non-Stationary Relationship between Autumn
765 Arctic Sea Ice and the Winter North Atlantic Oscillation. *Geophysical Research Letters*.

766 Kretschmer, M., Coumou, D., Agel, L., Barlow, M., Tziperman, E., and Cohen, J. (2018).
767 More-persistent weak stratospheric polar vortex states linked to cold extremes. *Bulletin*
768 *of the American Meteorological Society*, *99*(1), 49-60.

769 Laloyaux, P., de Boisseson, E., Balmaseda, M., Bidlot, J. R., Broennimann, S., Buizza, R., ...
770 and Kosaka, Y. (2018). CERA-20C: A coupled reanalysis of the Twentieth
771 Century. *Journal of Advances in Modeling Earth Systems*, *10*(5), 1172-1195.

772 Luo, D., Chen, Y., Dai, A., Mu, M., Zhang, R., and Ian, S. (2017). Winter Eurasian cooling
773 linked with the Atlantic multidecadal oscillation. *Environmental Research*
774 *Letters*, *12*(12), 125002.

775 Luo, D., Chen, X., Overland, J., Simmonds, I., Wu, Y., and Zhang, P. (2019). Weakened
776 potential vorticity barrier linked to recent winter Arctic sea-ice loss and mid-latitude
777 cold extremes. *Journal of Climate*, (2019).

McCusker, K. E., Fyfe, J. C., and Sigmond, M. (2016). Twenty-five winters of unexpected Eurasian cooling unlikely due to Arctic sea-ice loss. *Nature Geoscience*, *9*(11), 838.

Moore, G. W. K., and Renfrew, I. A. (2012). Cold European winters: interplay between the NAO and the East Atlantic mode. *Atmospheric Science Letters*, *13*(1), 1-8.

Mori, M., Kosaka, Y., Watanabe, M., Nakamura, H., and Kimoto, M. (2019). A reconciled estimate of the influence of Arctic sea-ice loss on recent Eurasian cooling. *Nature Climate Change*, *9*(2), 123.

Orsolini, Y. J., and Kvamstø, N. G. (2009). Role of Eurasian snow cover in wintertime circulation: Decadal simulations forced with satellite observations. *Journal of Geophysical Research: Atmospheres*, *114*(D19).

Orsolini, Y. J., Senan, R., Vitart, F., Balsamo, G., Weisheimer, A., and Doblas-Reyes, F. J. (2016). Influence of the Eurasian snow on the negative North Atlantic Oscillation in subseasonal forecasts of the cold winter 2009/2010. *Climate Dynamics*, *47*(3-4), 1325-1334.

Orsolini, Y., Wegmann, M., Dutra, E., Liu, B., Balsamo, G., Yang, K., ... and Senan, R. (2019). Evaluation of snow depth and snow-cover over the Tibetan Plateau in global reanalyses using in-situ and satellite remote sensing observations. *The Cryosphere*, 13, 2221–2239

Overland, J. E., Wood, K. R., and Wang, M. (2011). Warm Arctic—cold continents: climate impacts of the newly open Arctic Sea. *Polar Research*, *30*(1), 15787.

Overland, J. E., and Wang, M. (2018). Arctic-midlatitude weather linkages in North America. *Polar Science*, *16*, 1-9.

Pedersen, R. A., Cvijanovic, I., Langen, P. L., and Vinther, B. M. (2016). The impact of regional Arctic sea ice loss on atmospheric circulation and the NAO. *Journal of Climate*, *29*(2), 889-902.

Peings, Y., Brun, E., Mauvais, V., and Douville, H. (2013). How stationary is the relationship between Siberian snow and Arctic Oscillation over the 20th century?. *Geophysical Research Letters*, *40*(1), 183-188.

Peings, Y., Douville, H., Colin, J., Martin, D. S., and Magnusdottir, G. (2017). Snow–(N) AO teleconnection and its modulation by the Quasi-Biennial Oscillation. *Journal of Climate*, *30*(24), 10211-10235.

809 Peings, Y. (2019). Ural Blocking as a driver of early winter stratospheric
810 warmings. *Geophysical Research Letters*.

811 Petoukhov, V., and Semenov, V. A. (2010). A link between reduced Barents-Kara sea ice and
812 cold winter extremes over northern continents. *Journal of Geophysical Research:*
813 *Atmospheres*, *115*(D21).

814 Poli, P., Hersbach, H., Dee, D. P., Berrisford, P., Simmons, A. J., Vitart, F., ... and Trémolet,
815 Y. (2016). ERA-20C: An atmospheric reanalysis of the twentieth century. *Journal of*
816 *Climate*, *29*(11), 4083-4097.

817 Rayner, N. A. A., Parker, D. E., Horton, E. B., Folland, C. K., Alexander, L. V., Rowell, D.
818 P., ... and Kaplan, A. (2003). Global analyses of sea surface temperature, sea ice, and
819 night marine air temperature since the late nineteenth century. *Journal of Geophysical*
820 *Research: Atmospheres*, *108*(D14).

821 Robinson, David A., Estilow, Thomas W., and NOAA CDR Program (2012). NOAA Climate
822 Data Record (CDR) of Northern Hemisphere (NH) Snow Cover Extent (SCE), Version
823 1.

824 Rohrer, M., Brönnimann, S., Martius, O., Raible, C. C., Wild, M., and Compo, G. P. (2018).
825 Representation of extratropical cyclones, blocking anticyclones, and Alpine circulation
826 types in multiple reanalyses and model simulations. *Journal of Climate*, *31*(8), 3009-
827 3031.

828 Rohrer, M., Broennimann, S., Martius, O., Raible, C. C., and Wild, M. (2019). Decadal
829 variations of blocking and storm tracks in centennial reanalyses. *Tellus A: Dynamic*
830 *Meteorology and Oceanography*, *71*(1), 1-21.

831 Romanowsky, E., Handorf, D., Jaiser, R., Wohltmann, I., Dorn, W., Ukita, J., Cohen, J.,
832 Dethloff, K. and Rex, M. (2019). The role of stratospheric ozone for Arctic-midlatitude
833 linkages. *Scientific reports*, *9*(1), 7962.

834 Ruggieri, P., Kucharski, F., Buizza, R., and Ambaum, M. H. P. (2017). The transient
835 atmospheric response to a reduction of sea-ice cover in the Barents and Kara
836 Seas. *Quarterly Journal of the Royal Meteorological Society*, *143*(704), 1632-1640.

837 Saito, K., Cohen, J., and Entekhabi, D. (2001). Evolution of atmospheric response to early-
838 season Eurasian snow cover anomalies. *Monthly Weather Review*, *129*(11), 2746-2760.

839 Scaife, A. A., Arribas, A., Blockley, E., Brookshaw, A., Clark, R. T., Dunstone, N., ... and
840 Hermanson, L. (2014). Skillful long-range prediction of European and North American
841 winters. *Geophysical Research Letters*, *41*(7), 2514-2519.

842 Scaife, A. A., Karpechko, A. Y., Baldwin, M. P., Brookshaw, A., Butler, A. H., Eade, R., ...
843 and Smith, D. (2016). Seasonal winter forecasts and the stratosphere. *Atmospheric*
844 *Science Letters*, *17*(1), 51-56.

845 Scherrer, S. C., Croci-Maspoli, M., Schwierz, C., and Appenzeller, C. (2006). Two-
846 dimensional indices of atmospheric blocking and their statistical relationship with
847 winter climate patterns in the Euro-Atlantic region. *International Journal of*
848 *Climatology: A Journal of the Royal Meteorological Society*, *26*(2), 233-249.

849 Schwartz, C., and Garfinkel, C. I. (2017). Relative roles of the MJO and stratospheric
850 variability in North Atlantic and European winter climate. *Journal of Geophysical*
851 *Research: Atmospheres*, *122*(8), 4184-4201.

852 Schwierz, C., Croci-Maspoli, M., and Davies, H. C. (2004). Perspicacious indicators of
853 atmospheric blocking. *Geophysical research letters*, *31*(6).

854 Screen, J. A. (2017). Simulated atmospheric response to regional and pan-Arctic sea ice
855 loss. *Journal of Climate*, *30*(11), 3945-3962.

856 Screen, J. A., Deser, C., Smith, D. M., Zhang, X., Blackport, R., Kushner, P. J., ... and Sun, L.
857 (2018). Consistency and discrepancy in the atmospheric response to Arctic sea-ice loss
858 across climate models. *Nature Geoscience*, *11*(3), 155.

859 Smith, D. M., Scaife, A. A., Eade, R., and Knight, J. R. (2016). Seasonal to decadal prediction
860 of the winter North Atlantic Oscillation: emerging capability and future
861 prospects. *Quarterly Journal of the Royal Meteorological Society*, *142*(695), 611-617.

862 Sorokina, S. A., Li, C., Wettstein, J. J., and Kvamstø, N. G. (2016). Observed atmospheric
863 coupling between Barents Sea ice and the warm-Arctic cold-Siberian anomaly
864 pattern. *Journal of Climate*, *29*(2), 495-511.

865 Sun, C., Zhang, R., Li, W., Zhu, J., and Yang, S. (2019). Possible impact of North Atlantic
866 warming on the decadal change in the dominant modes of winter Eurasian snow water
867 equivalent during 1979–2015. *Climate Dynamics*, 1-11.

Suo, L., Gao, Y., Guo, D., Liu, J., Wang, H., and Johannessen, O. M. (2016). Atmospheric response to the autumn sea-ice free Arctic and its detectability. *Climate Dynamics*, *46*(7-8), 2051-2066.

Thompson, D. W., and Wallace, J. M. (1998). The Arctic Oscillation signature in the wintertime geopotential height and temperature fields. *Geophysical research letters*, *25*(9), 1297-1300.

Tibaldi, S., and Molteni, F. (1990). On the operational predictability of blocking. *Tellus A*, *42*(3), 343-365.

Trenary, L., and DelSole, T. (2016). Does the Atlantic Multidecadal Oscillation get its predictability from the Atlantic Meridional Overturning circulation?. *Journal of Climate*, *29*(14), 5267-5280.

Tyrrell, N. L., Karpechko, A. Y., and Räisänen, P. (2018). The influence of Eurasian snow extent on the northern extratropical stratosphere in a QBO resolving model. *Journal of Geophysical Research: Atmospheres*, *123*(1), 315-328.

Tyrrell, N. L., Karpechko, A. Y., Uotila, P., and Vihma, T. (2019). Atmospheric Circulation Response to Anomalous Siberian Forcing in October 2016 and its Long-Range Predictability. *Geophysical Research Letters*, *46*(5), 2800-2810.

Vihma, T. (2014). Effects of Arctic sea ice decline on weather and climate: A review. *Surveys in Geophysics*, *35*(5), 1175-1214.

Walsh, J. E., Fetterer, F., Scott Stewart, J., and Chapman, W. L. (2017). A database for depicting Arctic sea ice variations back to 1850. *Geographical Review*, *107*(1), 89-107.

Wang, L., Ting, M., and Kushner, P. J. (2017). A robust empirical seasonal prediction of winter NAO and surface climate. *Scientific reports*, *7*(1), 279.

Wanner, H., Brönnimann, S., Casty, C., Gyalistras, D., Luterbacher, J., Schmutz, C., ... and Xoplaki, E. (2001). North Atlantic Oscillation–concepts and studies. *Surveys in geophysics*, *22*(4), 321-381.

Warner, J. L. (2018). Arctic sea ice–a driver of the winter NAO?. *Weather*, *73*(10), 307-310.

Wegmann, M., Orsolini, Y., Vázquez, M., Gimeno, L., Nieto, R., Bulygina, O., ... and Sterin, A. (2015). Arctic moisture source for Eurasian snow cover variations in autumn. *Environmental Research Letters*, *10*(5), 054015.

Wegmann, M., Brönnimann, S., and Compo, G. P. (2017). Tropospheric circulation during the early twentieth century Arctic warming. *Climate dynamics*, *48*(7-8), 2405-2418.

Wegmann, M., Y. Orsolini, E. Dutra, O. Bulygina, A. Sterin, and S. Brönnimann, (2017). Eurasian snow depth in long-term climate reanalyses. Cryosphere, 11, 923–935

Wegmann, M., Orsolini, Y., and Zolina, O. (2018a). Warm Arctic− cold Siberia: comparing the recent and the early 20th-century Arctic warmings. *Environmental Research Letters*, *13*(2), 025009.

Wegmann, M., Dutra, E., Jacobi, H. W., and Zolina, O. (2018b). Spring snow albedo feedback over northern Eurasia: Comparing in situ measurements with reanalysis products. *Cryosphere*, *12*(6).

Xu, B., Chen, H., Gao, C., Zhou, B., Sun, S., and Zhu, S. (2019). Regional response of winter snow cover over the Northern Eurasia to late autumn Arctic sea ice and associated mechanism. *Atmospheric Research*, *222*, 100-113.

Yao, Y., Luo, D., Dai, A., and Simmonds, I. (2017). Increased quasi stationarity and persistence of winter Ural blocking and Eurasian extreme cold events in response to Arctic warming. Part I: Insights from observational analyses. *Journal of Climate*, *30*(10), 3549-3568.

Ye, K., & Wu, R. (2017). Autumn snow cover variability over northern Eurasia and roles of atmospheric circulation. *Advances in Atmospheric Sciences*, *34*(7), 847-858.

Yeo, S. R., Kim, W., and Kim, K. Y. (2017). Eurasian snow cover variability in relation to warming trend and Arctic Oscillation. *Climate dynamics*, *48*(1-2), 499-511.

Zhang, J., Tian, W., Chipperfield, M. P., Xie, F., and Huang, J. (2016). Persistent shift of the Arctic polar vortex towards the Eurasian continent in recent decades. *Nature Climate Change*, *6*(12), 1094.